



Discover Generics

Cost-Effective CT & MRI Contrast Agents



WATCH VIDEO

AJNR

Diffusion-Weighted MR Imaging of Global Cerebral Anoxia

Andres Arbelaez, Mauricio Castillo and Suresh K. Mukherji

AJNR Am J Neuroradiol 1999, 20 (6) 999-1007

<http://www.ajnr.org/content/20/6/999>

This information is current as
of June 15, 2025.

Diffusion-Weighted MR Imaging of Global Cerebral Anoxia

Andres Arbelaez, Mauricio Castillo, and Suresh K. Mukherji

BACKGROUND AND PURPOSE: Diffuse cerebral anoxia is a devastating event, and its acute findings, as revealed by conventional MR imaging and CT scanning, may be subtle. We analyzed diffusion-weighted and conventional MR images of patients with diffuse cerebral anoxia to determine their usefulness in establishing the diagnosis during the acute period and in determining the age of insult.

METHODS: We reviewed 11 MR imaging studies of 10 patients who had experienced prolonged cardiac arrest. All of the patients underwent echo-planar diffusion-weighted imaging with low- and high-strength B values and multiplanar unenhanced MR imaging. We considered bright areas on the high-strength diffusion-weighted images to be abnormal when compared with low-strength images. Special attention was given to the cortex, basal ganglia, thalami, hippocampi, cerebellum, and white matter. Conventional MR studies also were reviewed, and abnormalities noted. The medical records of all of the patients were reviewed.

RESULTS: Four patients who underwent imaging during the acute period (<24 hours) had bright basal ganglia (n = 2), bright cerebellum (n = 3), and bright cortex (n = 1) shown on their diffusion-weighted images. For these patients, conventional MR images showed questionable increased T2-weighted signal intensity in the basal ganglia (n = 1), and the results of two studies were judged to be normal. During the early subacute period (24 hours–13 days), four patients were studied, and were determined to have an abnormal cortex (n = 3) and basal ganglia (n = 2). For two of these patients, conventional MR images showed similar abnormalities, and the results of one study were normal. For two patients who underwent imaging during the late subacute period (14–20 days), diffusion-weighted images showed abnormalities mostly confined to white matter. Two patients who underwent imaging during the chronic phase (>21 days) had normal results of their diffusion-weighted imaging and one had evidence of laminar necrosis revealed by conventional MR imaging.

CONCLUSION: During the acute period, high-strength diffusion-weighted images showed the abnormal basal ganglia, cerebellum, and cortex to a better extent than did conventional MR images. During the early subacute period, gray matter abnormalities were seen on diffusion-weighted images. During the late subacute period, diffusion-weighted images showed mostly white matter abnormalities. During the chronic stage, the results of diffusion-weighted imaging were normal. Our findings suggest that diffusion-weighted images are helpful for evaluating and dating diffuse cerebral anoxia, and therefore aid in the determination of prognosis and management of these patients.

During the acute period after diffuse cerebral anoxia, the results of conventional MR imaging and CT scanning may be normal, or the images and scans may show only subtle abnormalities. The imaging findings of diffuse cerebral anoxia include

obscured gray-white matter junctions, abnormal appearance of deep gray matter nuclei, infarctions in regions between major arterial territories, and laminar necrosis (1–7). Because of its poor prognosis, a method that rapidly aids in the identification of diffuse cerebral anoxia is desirable. Positron emission tomography and single-photon emission tomography may be helpful in the diagnosis of diffuse cerebral anoxia, but may be difficult to perform in this group of sick patients. The use of diffusion-weighted MR imaging for the diagnosis of acute cerebral infarction has been described, but this imaging technique has not been used to ex-

Received September 9, 1998; accepted after revision January 5, 1999.

From the Department of Radiology, University of North Carolina School of Medicine, Chapel Hill, NC 27599.

Address reprint requests to M. Castillo, CB 7510, UNC-CH, Chapel Hill, NC 27599.

© American Society of Neuroradiology

TABLE 1: Findings on conventional MR imaging and diffusion-weighted imaging in patients with global cerebral anoxia.

	Acute (<24 hours)	Early Subacute (24 hrs–13 days)	Late Subacute (14–20 days)	Chronic (>21 days)
T1WI	None	Abn. cerebellum	None	Laminar necrosis
T2WI	Abn. basal ganglia	Abn. basal ganglia, cortex, & cerebellum	None	Abn. basal ganglia
DWI	Abn. cerebellum, basal ganglia, & cortex	Abn. cortex & basal ganglia	Abn. white matter	None

Note.—T1WI, T1-weighted images; T2WI, T2-weighted images; DWI, diffusion-weighted images; Abn, abnormal appearing.

amine patients with diffuse cerebral anoxia (4, 8–12). We analyzed diffusion-weighted and conventional MR images of patients with diffuse cerebral anoxia to determine which method best showed the changes of cerebral anoxia, and which best determined the age of the insult.

Methods

Ten patients (11 MR imaging studies) with histories of prolonged cardiac arrest (>6 minutes), who subsequently developed encephalopathy, were studied using conventional MR and diffusion-weighted imaging. Four studies (four patients) were obtained within 24 hours of initial insult (acute period), five studies (four patients) during the subacute period (24 hours–20 days), and two studies (two patients) during the chronic period (>21 days). All studies were conducted using a 1.5-T unit with echo-planar capabilities. Conventional unenhanced sagittal T1-weighted imaging was performed with 500–600/12–14/2 (TR range/TE range/excitations), a 5-mm section thickness, and axial and coronal proton density. Conventional fast spin-echo T2-weighted imaging was performed with 3000–4500/15, 93–105/1, 4-mm section thickness, echo train length of 7, and interecho spacing of 15 milliseconds. Diffusion-weighted imaging was performed in the axial projection with 0.8/123 (TR/TE), 6-mm section thickness, low-strength gradient (B: 30 s/mm²), and high-strength diffusion gradient (B: 1100 seconds/mm²) for acquisition times of 4.6 seconds per study. The low B value images served as a baseline for comparison with the high B value images. With our equipment, application of the diffusion gradient is restricted to the z axis (section selection).

Two neuroradiologists retrospectively, jointly, and without blinding reviewed both diffusion-weighted images and conventional MR studies. By consensus, they labeled as abnormal those areas in which the signal intensity was increased and was significantly different in the high-strength diffusion images when compared with the low-strength diffusion images. Special attention was given to the signal characteristics of the cortex, basal ganglia, thalami, hippocampi, cerebellum, and white matter. The abnormalities identified on the conventional MR images also were recorded and compared with those seen on the diffusion-weighted images. We also reviewed the patients' medical records to assess causes of hypoxic insult as well as their outcomes.

Results

We studied male patients only (age range, 2–63 years), and had experienced documented prolonged cardiac arrest (>6 minutes) that subsequently resulted in coma. Death occurred in six patients, and four remained in a vegetative state. The causes for the cardiac arrests were myocardial infarction (n =

6), sepsis (n = 2), cocaine overdose (n = 1), and electrocution (n = 1). A summary of the findings is provided in Table 1.

Acute Period

The acute period is less than 24 hours after insult. Four patients underwent imaging during the acute period. Three of them underwent imaging within 3 hours of cardiac arrest. For two of the three patients, the results of conventional MR studies were considered to be normal, but the diffusion-weighted images showed that the cerebellum was diffusely brighter than the cerebral hemispheres (Fig 1A and B). For one of these two patients, follow-up conventional MR images showed a diffusely swollen cerebellum, supratentorial cortex, and basal ganglia (Fig 1C and D). For the second patient with an abnormal cerebellum, a follow-up study was not conducted. For the third patient of this group, who also underwent imaging within 3 hours of cardiac arrest, the results of the conventional MR study were considered to be normal and the high-strength diffusion-weighted images showed increased signal intensity in the basal ganglia (Fig 2A). The fourth patient of this group underwent imaging 20 hours after insult, and a conventional MR study showed questionable increased signal intensity in the basal ganglia on proton density- and T2-weighted images (Fig 3A). The diffusion-weighted images confirmed this abnormality, and also showed abnormal hyperintensity in the perirolandic and occipital cortices, basal ganglia, and cerebellum (Fig 3B–E).

Subacute Period

The subacute period is from 24 hours through 20 days. Four patients underwent imaging during the subacute period, which is divided into early (24 hours–13 days) and late (14–20 days) stages. Three MR studies were conducted between 3 and 6 days after insult. For one of these patients, the results of the conventional MR study initially were judged to be normal, and the diffusion-weighted images showed abnormal hyperintensity, mostly in the cerebral cortex (Fig 4A and B). For the second patient in this group, the conventional MR study showed increased signal intensity in basal ganglia, thalami,

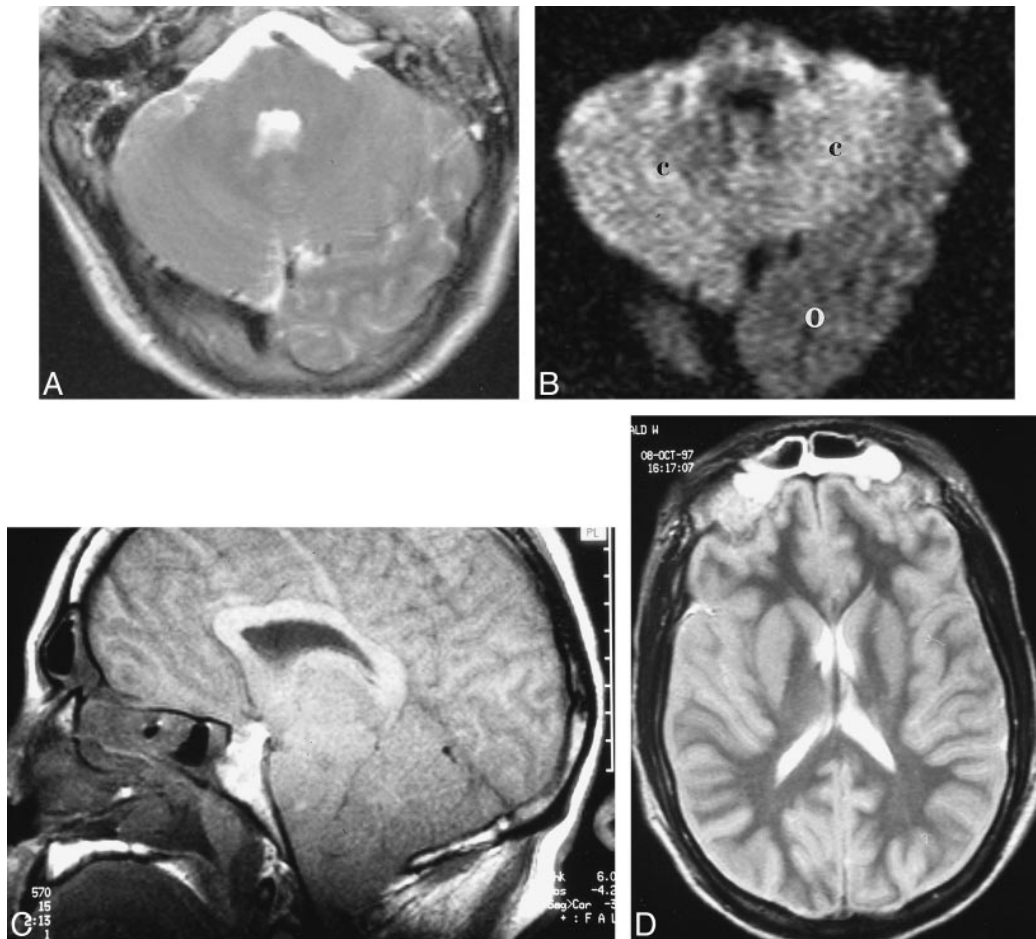


FIG 1. Bright cerebellum on diffusion-weighted images as the initial finding after cerebral anoxia.

A, Axial T2-weighted image, 3300/105/1 (TR/TE/excitations), obtained within 3 hours of cardiac arrest, shows the cerebellum to be of normal appearance.

B, Corresponding high-strength diffusion-weighted image, 0.8/123/1100 (TR/TE/B value), shows that the cerebellum (c) is diffusely bright when compared with the left occipital lobe (o).

C, Follow-up image obtained 3 days after anoxic episode. Midsagittal T1-weighted image (570/15/1) shows swollen cerebellum with upward transtentorial and downward transtentorial herniations. The fourth ventricle and brain stem are compressed.

D, Axial T2-weighted image (3500/93/1), obtained at same time as the image shown in C, shows swollen and bright cortex, effaced cortical sulci, and bright basal ganglia. Because of technical problems, diffusion-weighted images were not obtained as part of the follow-up study. This patient died.

hippocampi, and cortices on proton density- and T2-weighted images. For this patient, the deep gray matter structures and the cerebral cortex were also abnormally bright on the diffusion-weighted images. For the third patient in this group (who also underwent imaging during the acute period), the conventional MR study conducted 3 days after insult showed a bright basal ganglia and cerebral cortex (Fig 2B and C). The corresponding high-strength diffusion-weighted images confirmed these findings, revealed them better, and showed them to be more extensive than did the conventional MR images. This patient underwent a third follow-up study 14 days after cardiac arrest. This follow-up study showed no significant abnormality on the conventional MR images, but did reveal diffusely increased signal intensity in the white matter of the centra semiovale and posterior limbs of the internal capsules. Decreasing brightness in gray matter structures was also present on the high-strength dif-

fusion-weighted images (Fig 2E–G). The fourth patient in this group underwent imaging 20 days after insult, and the results of the conventional MR study were interpreted to be normal (Fig 5A). The high-strength diffusion-weighted images showed abnormal brightness in the centra semiovale and no definite abnormality in the gray matter (Fig 5B).

Chronic Period

The chronic period is 21 days and more. Two patients underwent imaging during the chronic period. For one patient, the results of the diffusion-weighted imaging performed 21 days after insult were judged to be normal. The conventional MR images showed residual increased T2-weighted signal intensity in the basal ganglia. For another patient, who underwent imaging 22 days after cardiac arrest, the conventional MR images showed linear hyperintensities in the cortex on T1-weighted im-

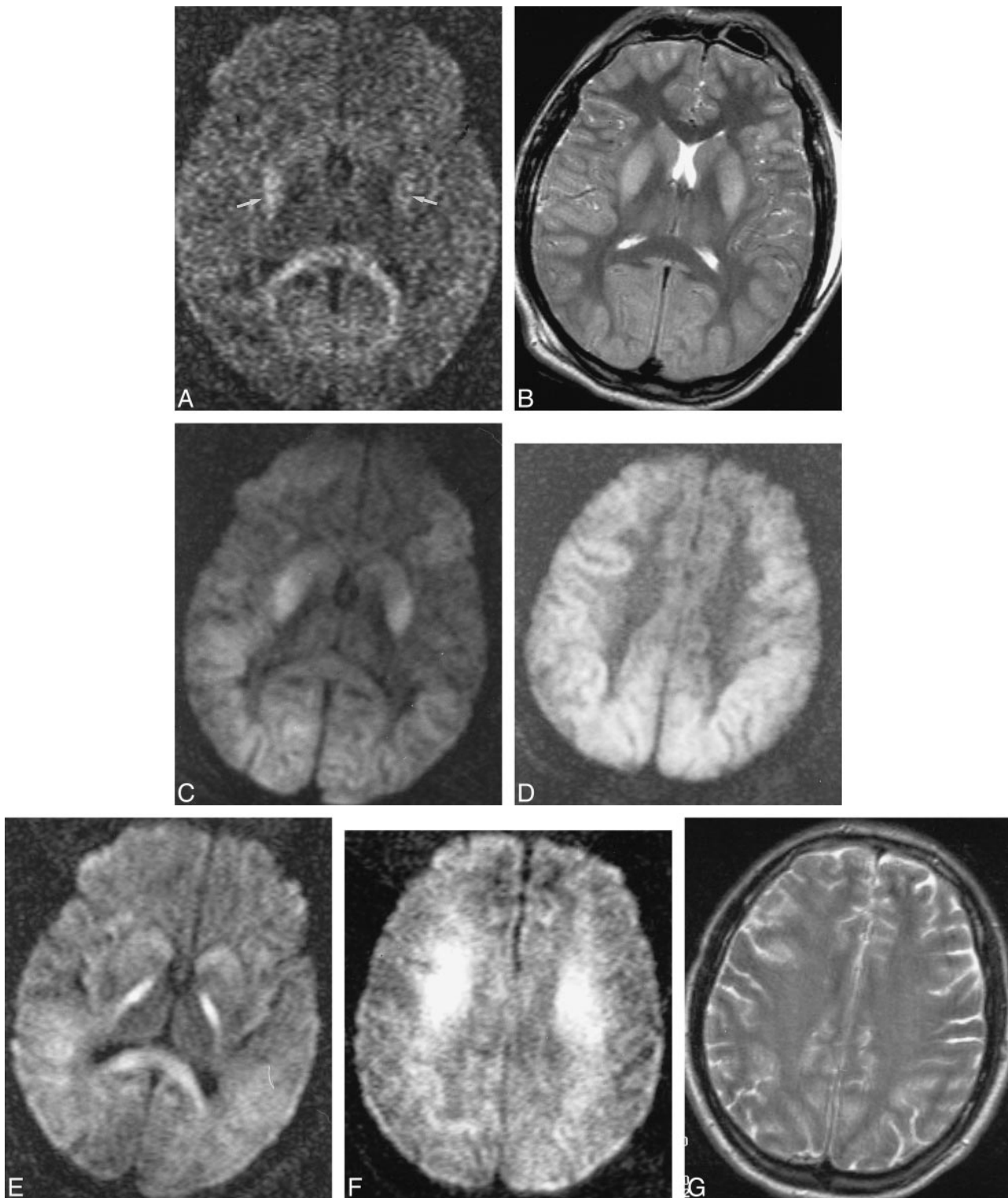


FIG 2. Sequential diffusion-weighted images show bright basal ganglia as the initial finding after anoxia.

A, Axial high-strength diffusion-weighted image (0.8/123/1100), obtained less than 3 hours after cardiac arrest (because of electrocution), shows abnormal brightness in lentiform nuclei (arrows). Brightness in splenium of corpus callosum is normal because transverse white matter fibers are perpendicular to the plane (z) in which the diffusion gradient was applied.

B, Axial T2-weighted image (4200/105/1), obtained 3 days after insult, shows increased signal intensity in basal ganglia and possibly in occipital cortices.

C, High-strength diffusion-weighted image (0.8/123/1100), obtained at same time as the image shown in B, reveals abnormally bright basal ganglia and cortex in frontal, posterior temporal, and occipital lobes.

D, High-strength diffusion-weighted image (0.8/123/1100), obtained at same time as the image shown in B, shows that the cortex in the frontal and parietal regions is abnormally bright.

E, High-strength diffusion-weighted image (0.8/123/1100), obtained 14 days after insult and corresponding to the image shown in C, reveals decreasing signal intensity from gray matter structures and abnormal brightness in posterior limb of internal capsules.

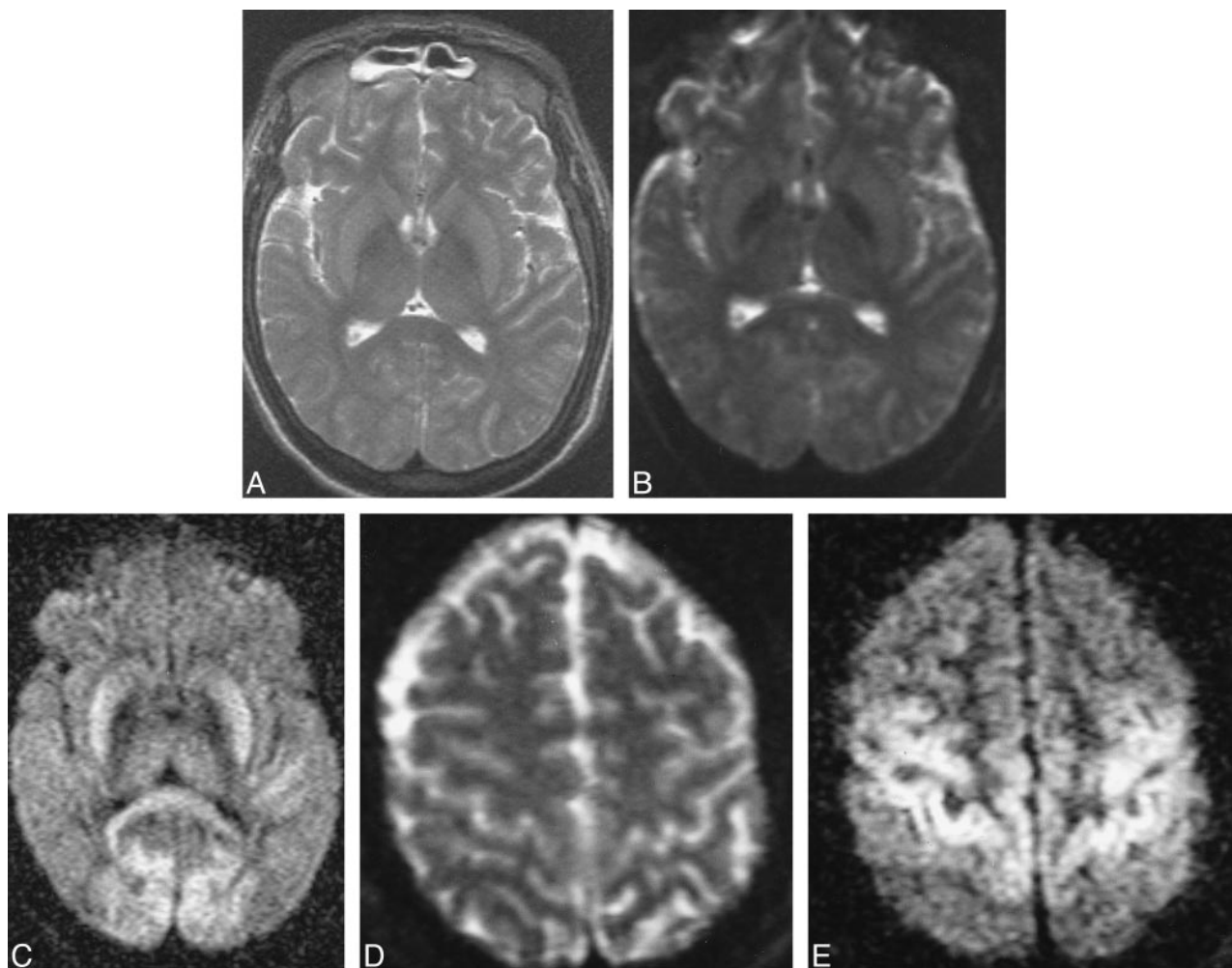


FIG 3. Bright basal ganglia and cortex on diffusion-weighted images obtained during the acute period (20 hours after insult).

A, Axial T2-weighted image (4500/105/1) shows questionable increased signal intensity in basal ganglia.

B, Corresponding low-strength diffusion-weighted image (0.8/123/30) shows no abnormality.

C, Corresponding high-strength diffusion-weighted image (0.8/123/1100) shows abnormally bright basal ganglia, thalami, and cortex (particularly in medial-occipital regions).

D, More cephalad axial low-strength diffusion-weighted image (0.8/123/30) shows no abnormality.

E, Corresponding high-strength diffusion-weighted image (0.8/123/1100) shows abnormally bright cortex surrounding the central sulci. This patient survived.

ages that were considered to represent laminar necrosis (Fig 6A). The results of proton density-, T2-, and diffusion-weighted imaging were judged to be normal (Fig 6B).

Discussion

Diffusion-weighted echo-planar MR imaging may show cerebral infarctions as early as 1 hour after occurrence (4, 8–10). In the normal brain, the extracellular compartment permits water molecules to move in a disorganized and random fashion (Brownian motion), resulting in phase shift loss and

relatively low signal intensity on high-strength diffusion-weighted images. Cytotoxic edema, as in early anoxic encephalopathy, leads to restriction of Brownian motion, producing high signal intensity on diffusion-weighted images. Whole-brain diffusion-weighted MR imaging is performed rapidly, and may be used in the evaluation of sick patients in whom the duration of conventional MR imaging leads to motion-related image degradation.

With our MR imaging units, we are able to perform whole-brain diffusion-weighted imaging in slightly longer than 4 seconds per study. Images are obtained with a low-diffusion value ($B = 30 \text{ s/}$

F, Axial high-strength diffusion-weighted image (0.8/123/1100), obtained at the same time as the image shown in E and at same level as the image shown in D, reveals decreasing signal intensity from the cortex and abnormal brightness in the centra semiovale.

G, Corresponding conventional T2-weighted image (4500/105/1) shows normal results. This patient survived.

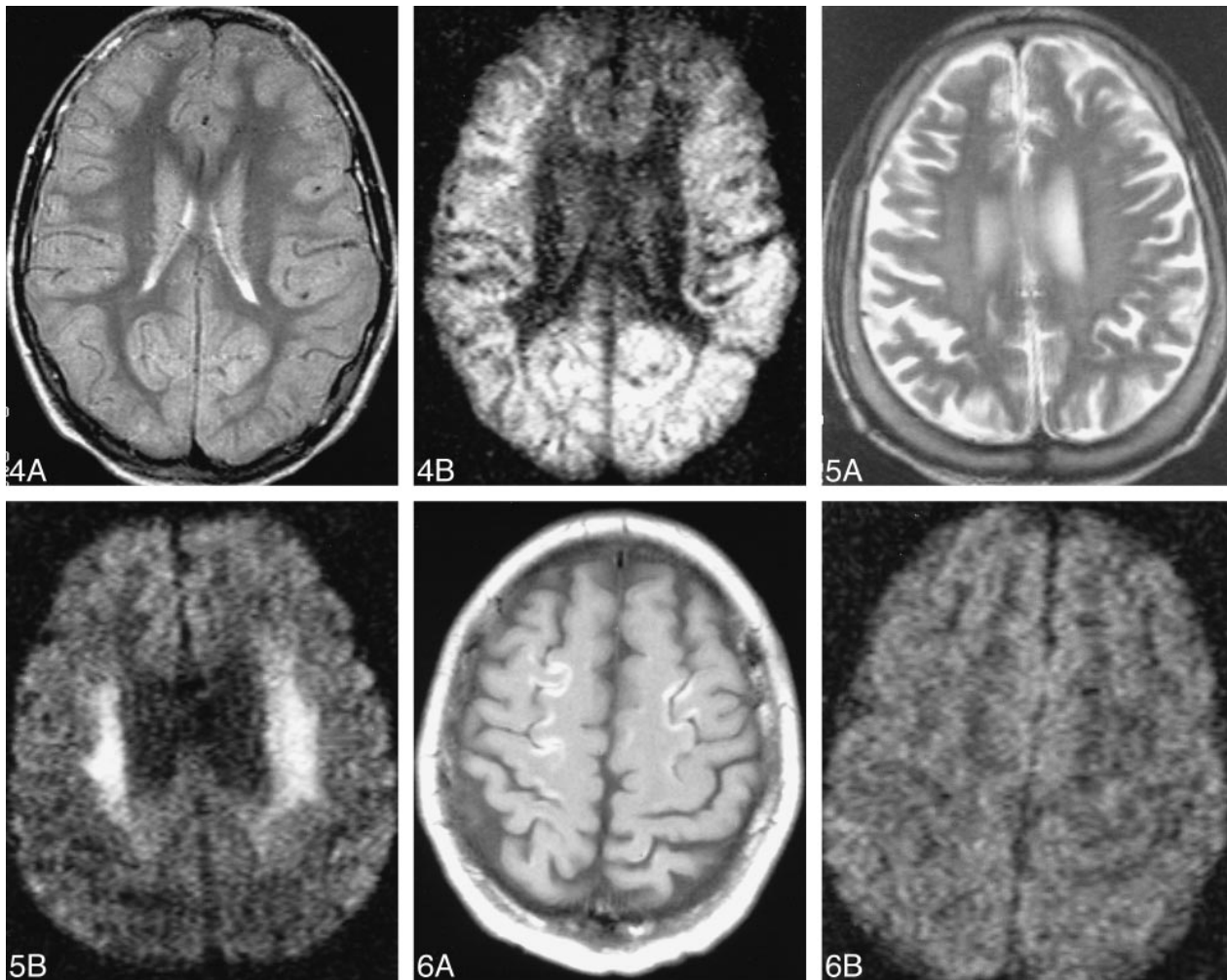


FIG 4. Abnormally bright cortex in the early subacute period.

A, Axial T2-weighted image (4500/105/1) initially was interpreted as normal. A careful retrospective analysis raised the possibility of increased signal intensity and thickening of the cortex.

B, Corresponding high-strength diffusion-weighted image (0.8/123/1100) shows abnormal brightness preferentially involving the cortex.

FIG 5. Images of abnormal white matter obtained during the late subacute period (15–20 days).

A, Axial T2-weighted image (3300/105/1) shows no definite abnormalities. There is subtle and nonspecific increased signal intensity in the white matter.

B, Corresponding high-strength diffusion-weighted image (0.8/123/1100) shows abnormally bright white matter in centra semiovale and no definite cortical abnormalities.

FIG 6. Images of laminar necrosis obtained during the chronic period.

A, Axial T1-weighted image (550/15/1) shows linear brightness along the superior frontal, pre-central, and central gyri corresponding to the sequelae of laminar necrosis 22 days after cardiac arrest.

B, Axial high-strength diffusion-weighted image (0.8/123/1100), obtained inferior to the image shown in A (convexity diffusion images were degraded by magnetic susceptibility artifacts), shows normal results.

mm²) and with a high-diffusion value ($B = 1100$ second/mm²). We use the low B value images as a baseline for comparison with the high B value images. Areas of increased signal in the high B value images, when compared with the low B value images, may be considered abnormal.

A lack of cerebral oxygenation leads to hypoxia and hypercapnia, resulting in increased blood flow as a compensatory mechanism (1, 13–19). Adequate levels of adenosine triphosphate and phosphocreatine may be maintained even with a 5% to 7% reduction in inhaled oxygen. Cerebral ischemia may be focal or global, and the latter is generally secondary to an abnormal cardiac function. After a

short period of ischemia, immediate cerebral reperfusion may prevent necrosis (1, 15, 16). Longer periods of ischemia (anoxia) lead to a decrease in adenosine triphosphate and phosphocreatine and an elevation of lactate, resulting in global cerebral injury (20–24). Factors that determine the degree of injury in cases of global cerebral ischemia include the duration of insult, degree of blood flow, temperature, and serum glucose levels (15, 16, 25–27). In adults, diffuse cerebral anoxia is generally caused by cardiac arrest, severe hypotension or hypertension, trauma, or venous sinus occlusion (2, 3, 13–15). In children, dehydration, neonatal anoxia, and child abuse are the most common causes.

Ischemic and anoxic encephalopathies have a poor prognosis.

The principle of "selective vulnerability" attempts to explain why different brain regions are affected in the presence of a diffuse insult such as generalized ischemia/anoxia (2, 15, 28). Predominantly gray matter damage is termed "selective neuronal necrosis" (2, 15, 29). An injury to neurons, glia, and blood vessels is termed "pan cerebral necrosis" (2, 15, 30). The capillary network is greater in gray matter than in white matter, reflecting their metabolism (1). Cerebral activity determines oxygenation, glucose metabolism, and blood flow by the mechanism of "local autoregulation" (15). The mechanism responsible for the coupling between local autoregulation and metabolism is not known, but the presence of hydrogen ions, adenosine, and nitric oxide may play a role (15, 31–33).

All of our patients suffered diffuse cerebral anoxia caused by prolonged cardiac arrests. For four of the patients, diffusion-weighted images obtained during the acute period (<24 hours after insult) showed increased signal intensity in the cortex (particularly perirolandic and occipital) ($n = 1$), basal ganglia ($n = 2$), and cerebellum ($n = 3$). For two of these patients, the results of conventional MR imaging were judged to be normal, and for two of the patients, the basal ganglia showed questionably increased proton density- and T2-weighted signal intensity. Prior investigations have shown that the regions affected in hypoxic patients are injured during acute global cerebral ischemia (15, 28). Layers 3, 4, and 5 of the cortex are sensitive to ischemia, and may become necrotic ("laminar necrosis") (2, 3, 5, 15, 28). Additionally, the watershed zones and the hippocampi (particularly the cornu Ammonis 1 zone) also are prone to damage from global ischemia (1, 4, 6, 7, 28). The vulnerability of these gray matter regions can be attributed to a combination of abnormal blood flow, basal metabolic rate, and presence of receptors for excitatory amino acids. Overstimulation by excitatory substances, such as glutamate, also may help to explain selective neuronal necrosis (1, 6, 7, 11, 15, 29, 34–37). Ischemia leads to the release of glutamate, and because most receptors for this substance are located in the dendrites, the gray matter is affected first and more severely. Glutamate leads to alterations in ionic homeostasis and results in cytotoxic edema (1, 15, 16, 38). In turn, cytotoxic edema leads to restriction of extracellular water motion and increased signal intensity in high-strength diffusion-weighted images, as seen in the cases of our patients. Therefore, the abnormalities seen in our patients during the acute period correlate well with the regions that prior investigators have shown to be affected initially. The abnormalities were seen earlier and to a better extent on diffusion-weighted than on conventional MR images. It is possible that before cytotoxic edema reaches the degree needed to become visible on conventional MR images, there is microscopic re-

striction of extracellular water motion leading to increased signal intensity on diffusion-weighted images. This would explain why some areas are abnormally bright on diffusion-weighted images but normal or nearly normal on conventional MR images.

Four patients underwent imaging during the subacute period (24 hours–20 days). Diffusion-weighted images obtained during the early subacute period (24 hours–13 days) showed a bright cortex and basal ganglia, findings that may be explained by similar mechanisms to those seen during the acute period. The findings also were shown by two of the conventional MR studies. During the subacute period, there is reperfusion of ischemic brain regions. Unfortunately, this mechanism is generally heterogeneous and insufficient for the reestablishment of normal cerebral blood flow because of underlying edema and increased viscosity of red blood cells (1, 39–43). This type of insufficient reperfusion is thought to increase cytotoxic edema in the affected areas (24, 44–47), and thus, in combination with the presence of vasogenic edema, it could further compromise extracellular water motion. The combination of increased cytotoxic and vasogenic edema leading to a restriction of Brownian motion results in increased signal intensity in the gray matter, as seen on conventional and diffusion-weighted images, respectively, during the subacute period. In addition, the phenomenon of "late neuronal death" (7, 11, 15, 37, 48), which predominantly affects the neocortex, hippocampi, and basal ganglia, also may contribute to the abnormalities present on conventional T2-weighted and diffusion-weighted images during the subacute period.

Two patients underwent imaging during the late subacute period (14–20 days). The diffusion-weighted images showed diffusely bright white matter, a finding that was not as obvious on the conventional MR images. Several mechanisms may explain this finding. With pancerebral necrosis, there is an alteration in the pH value, which contributes to the damage of glial cells (10, 16, 49, 50). This decreased pH value is caused by an increased production of lactate acid and to liberation of protons from hydrolysis of adenosine triphosphate (33). In a similar fashion to the mechanism of injury for gray matter already addressed, white matter may be injured by the release of excitatory substances resulting from global ischemia. Glutamate migrates via synaptic clefts in the gray matter to reach receptors located in glial cells (30, 51, 52). Other mechanisms that injure white matter as a result of anoxia include abnormal axoplasmic transport, abnormal action potentials, alteration of the sodium-potassium pump, and a process similar to Wallerian degeneration (Wallerian-like degeneration) (30, 53–55). Wallerian-like degeneration results in edema of neurofilaments, and also may contribute to limiting Brownian motion and lead to an increased signal intensity on high-strength diffusion-weighted images. One of our patients pre-

sented us with the unique opportunity to evaluate serial findings after global anoxia. Acutely, he had basal ganglia abnormality that 2 days later progressed to involve the cortex and that 14 days after insult involved the white matter (Fig 2). Because these abnormalities occur mostly at a cellular level, the findings are more evident on diffusion-weighted images than on conventional MR images.

For two patients studied during the chronic period (at 21 and 22 days), the results of the diffusion-weighted imaging were normal. One patient had evidence of laminar necrosis shown by conventional MR imaging. For the second patient, the results of conventional MR imaging were unremarkable. During the chronic period, cellular death and destruction of axons occur (2, 15, 54–57). This may lead to an increase in extracellular space, cavitation, and a greater freedom of Brownian motion, thus resulting in decreased signal intensity in the high B value diffusion-weighted images.

A potential pitfall in the interpretation of the results of diffusion-weighted MR imaging of patients with diffuse cerebral abnormalities caused by anoxia is related to the filming of the studies. If the cortex and basal ganglia are abnormally bright, it is conceivable that a technologist may set the window levels to compensate for this, and the results of the study may appear normal. This could occur with patients during the transition between the acute and subacute stages. A caveat in our study refers to the diffusion-weighted imaging sequence used. In our studies, because of intrinsic equipment limitations, the diffusion-weighted imaging was performed using a diffusion gradient only in the z-axis direction. It is possible that better characterization of infarcts may be obtained using multiplanar diffusion-weighted images and construction of apparent diffusion coefficient maps. For practical purposes, water motion during infarction is random and without vector, and should be visible regardless of the direction in which the diffusion gradient was applied.

Conclusion

For our patients, diffusion-weighted images showed earlier and more extensive abnormalities than did conventional MR images after global cerebral anoxia. In addition, cerebral abnormalities, as seen on diffusion-weighted images, followed sequential changes, with predominantly gray matter abnormalities during the acute and early subacute periods, white matter abnormalities during the late subacute period, and a return to normal during the chronic stage. This sequence of events is in accordance with that recently described for lobar infarctions seen on diffusion-weighted images (58). The diffusion abnormalities correlate well with known histologic abnormalities and underlying pathologic mechanisms occurring with global cerebral anoxia. We suggest that, in the presence of global cerebral anoxia, diffusion MR imaging should be the initial

imaging study used, and it is helpful in establishing the diagnosis, prognosis, and management of these patients.

References

1. TerPenning B. **Pathophysiology of stroke.** *Neuroimaging Clin N Am* 1992;2:389–408
2. Osborn AG. **Diagnostic Neuroradiology.** St. Louis: Mosby, 1994: 330–398
3. Castillo M. **Neuroradiology Companion. Methods, Guidelines and Imaging Fundamentals.** Philadelphia: JB Lippincott, 1995: 66–67
4. Castillo M. **Imaging of cerebral infarction.** *Curr Probl Diagn Radiol* 1998;27:105–132
5. Takahoshi S, Higano S, Ishii K. **Hypoxic brain damage. Cortical laminar necrosis and delayed changes in white matter at sequential MR imaging.** *Radiology* 1993;189:449–456
6. Barkovich AJ. **Pediatric Neuroimaging.** New York: Raven Press, 1995:113–145
7. Rivkin MJ, Volpe JJ. **Hypoxic-ischemic brain injury in the newborn.** *Semin Neurol* 1993;13:30–39
8. Castillo M, Mukherji SK. **Practical applications of diffusion magnetic resonance imaging in acute cerebral infarction.** *Emerg Radiol* 1997;4:249–254
9. Chien D, Kwong KK, Gress DR, Buonanno FS, Buxton RB, Rosen BR. **MR diffusion imaging of cerebral infarctions in humans.** *AJNR Am J Neuroradiol* 1992;13:1097–1102
10. Gray L, MacFall J. **Overview of diffusion imaging.** *Magn Reson Imaging Clin N Am* 1998;6:125–138
11. Beauchamp NJ, Bryan RN. **Acute cerebral ischemic infarction. A pathophysiologic review and radiologic perspective.** *AJR Am J Roentgenol* 1998;171:73–84
12. MacFall JR, Maki JH, Johnson GA, Heldund L, Benveniste H, Copher G. **Diffusion/microcirculation MRI in the rat brain.** *Magn Reson Med* 1991;19:305–310
13. Guyton AC, Hall JE. **Textbook of Medical Physiology. Cerebral Blood Flow, the Cerebrospinal Fluid, and Brain Metabolism.** Philadelphia: WB Saunders, 1996:563–789
14. Braunwald E. **Hypoxia, polycythemia and cyanosis.** In: Isselbacher KJ, Braunwald E, Wilson JD, Martin JB, Fauci AS, Kasper DL, eds. *Harrison's Principles of Internal Medicine.* 13th ed. New York: McGraw-Hill, 1994:178–181
15. Auer RN, Benveniste H. **Hypoxia and related condition.** In: Graham DT, Lantos PL, eds. *Greenfield's Neuropathology.* London: Arnold, 1997:263–314
16. Hossmann KA, Hoehn-Berlage M. **Diffusion and perfusion MR imaging of cerebral ischemia.** *Cerebrovasc Brain Metab Rev* 1995;7:187–217
17. Berntman L, Carlsson C, Siesjö BK. **Cerebral oxygen consumption and blood flow in hypoxia. Influence of sympathoadrenal activation.** *Stroke* 1979;10:20–25
18. Kozniowska E, Weller L, Hoper J, et al. **Cerebrocortical microcirculation in different stages of hypoxic hypoxia.** *J Cereb Blood Flow Metab* 1987;7:464–470
19. Berntman L, Dahlgren N, Siesjö BK. **Cerebral oxygen consumption and blood flow in the rat brain during extreme hypercapnia.** *Anesthesiology* 1979;50:299–305
20. Bizzi A, Righini A, Turner R, et al. **MR of diffusion slowing in global cerebral ischemia.** *AJNR Am J Neuroradiol* 1993;14: 1347–1354
21. Behar KL, Rothman DL, Hossmann KA. **NMR spectroscopic investigation of the recovery of energy and acid-base homeostasis in the cat brain after prolonged ischemia.** *J Cereb Blood Flow Metab* 1989;9:655–665
22. Gadian DG, Frackowiak RSJ, Crockard HA, et al. **Acute cerebral ischemia. Concurrent changes in cerebral blood flow, energy metabolism, pH and lactate measured with H₂ clearance and P-31 and H-1 nuclear magnetic resonance spectroscopy.** *J Cereb Blood Flow Metab* 1987;7:199–206
23. Nishijima MK, Koehler RC, Hurn PD, et al. **Posts ischemic recovery rate of cerebral ATP, phosphocreatine, pH and evoked potentials.** *Am J Physiol* 1989;257:1860–1870
24. Busza AL, Allen KL, King MD, van Bruggen N, Williams SR, Gadian DG. **Diffusion-weighted imaging studies of cerebral ischemia in gerbils.** *Stroke* 1992;23:1602–1613

25. Busto R, Dietrich WD, Globus MY, Ginsberg MD. **The importance of brain temperature in cerebral ischemic injury.** *Stroke* 1989;20:1113-1114
26. Siesjö BK, Katsura K, Møllergård P, Ekholm A, Lundgren J, Smith ML. **Acidosis-related brain damage.** *Prog Brain Res* 1993;96:23-48
27. Longstreth WT Jr, Diehr P, Cobb LA, et al. **Neurologic outcome and blood glucose levels during out-of-hospital cardiopulmonary resuscitation.** *Neurology* 1986;36:1186-1191
28. Cole G, Cowie VA. **Long survival after cardiac arrest. Case report and neuropathological findings.** *Clin Neuropathol* 1987;6:104-109
29. Rothman SM, Olney JW. **Glutamate and the pathophysiology of hypoxic/ischemic brain damage.** *Ann Neurol* 1986;19:105-111
30. Gehrman J, Kreutzberg G. **Microglia in experimental neuropathology.** In: Kettenmann H, Ransom BR, eds. *Neuroglia*. New York: Oxford University Press, 1995:883-904
31. Phillis JW, DeLong RE, Towner JK. **Adenosine deaminase inhibitors enhance cerebral anoxic hyperemia in the rat.** *J Cereb Blood Flow Metab* 1995;5:295-299
32. Hylland P, Nilsson GE, Lutz PL. **Time course of anoxia-induced increase in cerebral blood flow rate in turtles: evidence for a role of adenosine.** *J Cereb Blood Flow Metab* 1994;14:877-881
33. Paschen W, Djuricic B, Mies G, et al. **Lactate and pH in the brain. Association and dissociation in different pathophysiological states.** *J Neurochem* 1987;48:154-159
34. Garcia JH. **Morphology of global cerebral ischemia.** *Crit Care Med* 1989;16:979-987
35. Benveniste H, Drejer J, Schousboe A, Diemer NH. **Elevation of the extracellular concentrations of glutamate and aspartate in rat hippocampus during transient cerebral ischemia monitored by intracerebral microdialysis.** *J Neurochem* 1984;43:1369-1374
36. McDonald JW, Johnston MV. **Physiological and pathophysiological roles of excitatory amino acids during central nervous system development.** *Brain Res Rev* 1990;15:41-70
37. Siesjö BK, Zhao Q, Pahlmark K, Siesjö P, Katsura K, Folbergrova J. **Glutamate, calcium, and free radicals as mediators of ischemic brain damage.** *Ann Thorac Surg* 1995;59:1316-1320
38. Hansen AJ. **Effect of anoxia on ion distribution in the brain.** *Physiol Rev* 1985;65:101-148
39. Fischer EG. **Impaired perfusion following cerebrovascular stasis. A review.** *Arch Neurol* 1973; 29:361-366
40. Hossmann KA. **Hemodynamics of post-ischemic reperfusion of the brain.** In: Weinstein PR, ed. *Protection of the Brain from Ischemia*. Baltimore: Williams & Wilkins, 1990:21-36
41. Schuier FJ, Hossmann KA. **Experimental brain infarcts in cats. II. Ischemic brain edema.** *Stroke* 1980;11:593-601
42. Ginsberg MD, Budd WW, Welsh FA. **Diffuse cerebral ischemia in the cat. I. Local blood flow during severe ischemia and recirculation.** *Ann Neurol* 1978;3:482-492
43. Chiang J, Kowada M, Ames A, et al. **Cerebral ischemia. III. Vascular changes.** *Am J Pathol* 1968;52:455-476
44. Ginsberg MD, Welsh FA, Budd WW. **Abnormalities of brain blood flow and metabolism during recovery from diffuse cerebral ischemia. Dependence upon duration of ischemia.** *Acta Neurol Scand* 1977;56:126-128
45. Ito U, Ohno K, Nakamura R, et al. **Brain edema during ischemia and after restoration of blood flow.** *Stroke* 1979;10:542-547
46. Bell BA, Symon L, Branston NM. **CBF and time thresholds for the formation of ischemic cerebral edema, and effect of reperfusion in baboons.** *J Neurosurg* 1985;62:31-41
47. Hatashita S, Hoff JT. **Biomechanics of brain edema in acute cerebral ischemia in cats.** *Stroke* 1988;19:91-97
48. Abe K, Aoki M, Kawagoe J, et al. **Ischemic delayed neuronal death. A mitochondrial hypothesis.** *Stroke* 1995;26:1478-1489
49. Raichle ME. **The pathophysiology of brain ischemia.** *Ann Neurol* 1983;13:2-10
50. Hossmann KA. **Resuscitation potentials after prolonged global cerebral ischemia in cats.** *Crit Care Med* 1988;16:964-971
51. Sontheimer H, Kettenmann H, Backus KH, Schachner M. **Glutamate opens Na/K channels in cultured astrocytes.** *Glia* 1988;1:328-336
52. Blankenfeld G, Enkvist K, Kettenmann. **Gamma-aminobutyric acid and glutamate receptors.** In: Kettenmann H, Ransom BR, eds. *Neuroglia*. New York: Oxford University Press, 1995:335-345
53. Kimelberg HK. **Brain edema.** In: Kettenmann H, Ransom BR, eds. *Neuroglia*. New York: Oxford University Press, 1995:919-935
54. Stys PK, Ransom BR, Black JA, Waxman SG. **Anoxic/ischemic injury in axons.** In: Waxman SG, Kocsis JD, Stys PK, eds. *The Axon. Structure, Function and Pathophysiology*. New York: Oxford University Press, 1995:462-479
55. Griffin JW, George EB, Hsieh ST, Glass JD. **Axonal degeneration and disorders of the axonal cytoskeleton.** In: Waxman SG, Kocsis JD, Stys PK, eds. *The Axon. Structure, Function and Pathophysiology*. New York: Oxford University Press, 1995:375-390
56. Kuhn MJ, Mikulis DJ, Ayoub DM, Kosofsky BE, Davis KR, Taveras JM. **Wallerian degeneration after cerebral infarction: evaluation with sequential MR imaging.** *Radiology* 1985;172:179-182
57. Rabin BM, Hebel DJ, Salamon-Murayama N, Russell EJ. **Distal neuronal degeneration caused by intracranial lesions.** *AJR Am J Roentgenol* 1998;171:95-102
58. Burdette JH, Ricci RE, Pettiti N, Elster AD. **Cerebral infarction. Time course of signal intensity changes on diffusion-weighted MR imaging.** *AJR Am J Roentgenol* 1998;171:791-795